360° Switched Beam SIW Horn Arrays at 60 GHz, Phase Centers, and Friis Equation

Prabhat Baniya and Kathleen L. Melde
Department of Electrical and Computer Engineering
University of Arizona
Tucson, AZ, USA
pbaniya@arizona.edu; melde@arizona.edu

***Abstract*—The link model of switched beam horn arrays at 60 GHz based on the substrate integrated waveguide (SIW) technology with 360° angular coverage is presented. Each array has eight identical printed horn elements. The elements are oriented 45° relative to one another and can be individually excited to produce eight endfire beams in the horizontal plane. The over-the-air (OTA) transmission coefficients are measured and simulated between two arrays, in the line-of-sight (LoS) and non-LoS (NLoS) directions. The phase centers (PCs) of the excited elements are determined from post-processing optimization of simulated far-fields and incorporated in the Friis equation to accurately model the transmission.**

I. Introduction

Switched beam antennas at 60 GHz can provide multi-Gbps reconfigurable wireless communication at short range. They are low profile and small enough to be chip-integrated, allowing wireless interconnection between chips on a multichip module (MCM). The switchable beams provide one-to-many dynamic links between a chip and its surrounding neighbors [1]. Fixed beam antennas have been designed to establish static wireless links [2], [3] between chips. Their use is limited in the MCMs where connections between chips in many different directions need to be individually and dynamically established. Switched beam arrays have been demonstrated in [4]–[6] but without the full 360° coverage. In order to maximize signal and minimize interference, each beam should have high gain in its line-of-sight (LoS) direction and low gain in the non-LoS (NLoS) directions. In this paper, the Friis equation is used to accurately model the transmission between two switched beam substrate integrated waveguide (SIW) horn arrays in the LoS and NLoS directions, by considering the effect of the phase centers (PCs) [7]. The PC of an antenna is the point from which the radiation spreads spherically outward. The PC varies with angular section of the radiation pattern. The PCs are found from simulation and utilized in the Friis equation to model the over-the-air (OTA) transmission.

II. Switched Beam SIW Horn Arrays

Fig. 1 shows the switched beam SIW horn array consisting of eight identical printed horn elements oriented 45° relative to one another [8], [9]. Each element can be individually excited to produce eight endfire beams (i.e., $\phi_0 = 0°, \pm 45°, \pm 90°, \pm 135°, 180°$) in the horizontal plane, providing full 360° coverage. The array is targeted for use in chip-to-chip communications where each chip communicates with its eight neighbors [1]. As shown in Fig. 1, there are periodic metal strips with gradually increasing gaps and decreasing widths, on the flaring of the horn elements, printed on a 0.8 mm thick Rogers RT/duroid 5880 substrate ($\epsilon_r = 2.2, \tan\delta = 0.0009$). They serve to improve both the impedance and gain bandwidth. The flaring is quadratically tapered over the length to reduce the overall aperture reflections. The leaky-wave radiation from the strips improve the LoS gain while reducing the NLoS gain [10]. The via walls improve isolation between the elements since the ratio $p/d < 2$, where p and d are the via period length and diameter, respectively. The leakage losses are minimized and interelement coupling is reduced. The elements are fed through the conductor backed coplanar waveguide (CB-CPW)-to-SIW transitions [8]. Most of the radiation of the array is vertically polarized (E_θ).

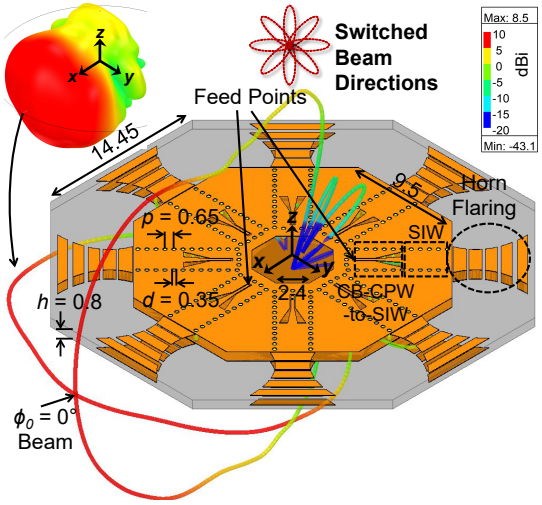

Fig. 1. 3-D model of the switched beam SIW horn array with integrated feed and 60 GHz 3-D gain pattern. All dimensions are in mm [8].

III. Measurement, Simulation, and Modeling

The fabricated PCB prototypes of the SIW horn arrays with the measurement setup are shown in Fig. 2. The OTA transmission coefficient ($|S_{21}|$) measurements are made in the LoS ($\phi = 0°$) and a NLoS ($\phi = 45°$) directions by landing 250 μm pitch ground-signal-ground probes on the CB-CPW

pads. The arrays are placed on a thick foam platform as it emulates air and separated center-to-center by 87.4 mm.

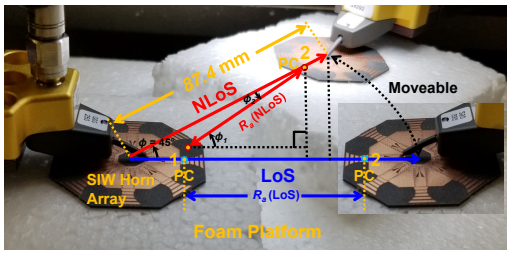

Fig. 2. Fabricated SIW horn arrays set up for OTA measurements.

For the LoS case, the probed horn elements of the two arrays are directly facing one another and their axes are aligned. The measured and simulated LoS $|S_{21}|$ i.e., $|S_{\text{LoS}}|$ are shown in Fig. 3(a). For the NLoS case, the axes of the probed horn elements make an angle of 45° at the center of array 1. The NLoS $|S_{21}|$ i.e., $|S_{\text{NLoS}}|$ are shown in Fig. 3(a). The simulated results are obtained by performing full-wave simulation of the two arrays in High Frequency Structural Simulator (HFSS).

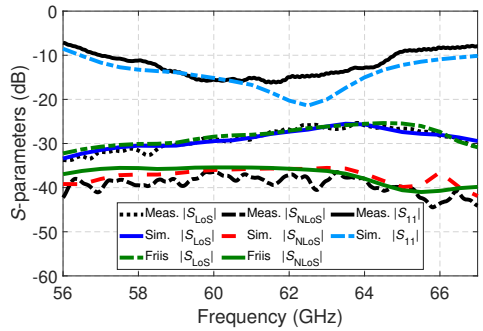

(a)

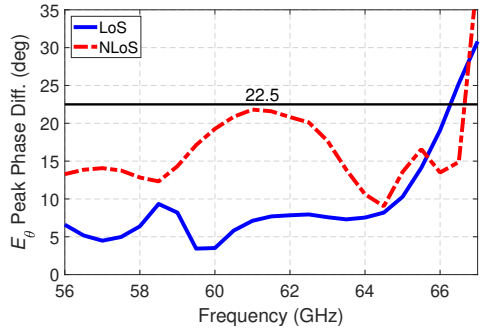

(b)

Fig. 3. (a) Measured, simulated, and model transmission coefficients (dB). (b) Simulated E_θ peak phase difference.

The Friis equation can be used to model the $|S_{21}|$ in a specific direction, given the angle-dependent realized gains $G_1(\phi_1)$ and $G_2(\phi_2)$ of the two antennas as follows [11]:

$$|S_{21}|^2 = \left(\frac{\lambda}{4\pi R_a}\right)^2 G_1(\phi_1)G_2(\phi_2) \tag{1}$$

where λ is the free-space wavelength, ϕ_1 and ϕ_2 are the angles made by the elements' axes with the line joining their PCs, and R_a is the distance between the PCs of the two elements, as shown in Fig. 2. The PCs are found from post-processing optimization of the full-wave simulation results of an array. The PCs for the LoS case is found by minimizing the peak phase difference (acceptable up to 22.5°) of E_θ within the 3-dB beamwidth angular range (i.e., $-40° \leq \phi \leq 40°$) of the main beam (in the horizontal plane), at most of the frequencies [see Fig. 3(b)]. This resulted in $R_a = 62.7$ mm, and $\phi_1 = \phi_2 = 0°$. For the NLoS case, the PC of element 2 is the same as the LoS case (relative to its array center, see Fig. 2) while the PC of element 1 is found by minimizing the peak phase difference within a new angular range $35° \leq \phi \leq 55°$ [see Fig. 3(b)]. This resulted in $R_a = 58.7$ mm, $\phi_1 = 54°$, and $\phi_2 = 9°$. Next, $G_1(\phi_1)$ and $G_2(\phi_2)$ are obtained directly from the HFSS simulation of the array. The Friis model results are included in Fig. 3(a) and show good agreement with measured and simulated results. The Friis model reduces computational memory and time since it only requires a full-wave simulation of a single array for link modeling in any direction. Only the post-processing optimizations (computationally simpler) are additionally needed to find the PCs (i.e., R_a, ϕ_1, ϕ_2) for each direction of interest.

ACKNOWLEDGEMENT

This work was supported by the US National Science Foundation under Grant ECCS-1708458.

REFERENCES

[1] P. Baniya and K. L. Melde, "Switched-beam endfire planar array with integrated 2-D Butler matrix for 60 GHz chip-to-chip space-surface wave communications," *IEEE Antennas Wireless Propag. Lett.*, vol. 18, no. 2, pp. 236–240, Feb. 2019.

[2] T. H. Jang, H. Y. Kim, S. H. Kim, D. M. Kang, and C. S. Park, "120 GHz on-board chip-to-chip wireless link using Y-shaped open-ended microstrip antenna," *IEEE Antennas Wireless Propag. Lett.*, vol. 18, no. 10, pp. 2165–2169, Oct. 2019.

[3] Y. Al-Alem, A. A. Kishk, and R. M. Shubair, "One-to-two wireless interchip communication link," *IEEE Antennas Wireless Propag. Lett.*, vol. 18, no. 11, pp. 2375–2378, Nov. 2019.

[4] Y. Li and K.-M. Luk, "A multibeam end-fire magnetoelectric dipole antenna array for millimeter-wave applications," *IEEE Trans. Antennas Propag.*, vol. 64, no. 7, pp. 2894–2904, Jul. 2016.

[5] B. Sadhu *et al.*, "A 250-mW 60-GHz CMOS transceiver SoC integrated with a four-element AiP providing broad angular link coverage," *IEEE J. Solid-State Circuits*, vol. 55, no. 6, pp. 1516–1529, Oct. 2020.

[6] I. M. Mohamed and A. Sebak, "60 GHz 2-D scanning multibeam cavity-backed patch array fed by compact SIW beamforming network for 5G applications," *IEEE Trans. Antennas Propag.*, vol. 67, no. 4, pp. 2320–2331, Apr. 2019.

[7] E. G. Plaza, G. Leon, S. Loredo, and L. F. Herran, "Calculating the phase center of an antenna: A simple experimental method based on linear near-field measurements. [measurements corner]," *IEEE Antennas Propag. Mag.*, vol. 59, no. 5, pp. 130–175, Oct. 2017.

[8] P. Baniya and K. L. Melde, "Switched beam SIW horn arrays at 60 GHz for 360° chip-to-chip communications," in *2021 IEEE Radio Wireless Symp. (RWS)*, San Diego, CA, USA, in press.

[9] P. Baniya and K. L. Melde, "Switched beam SIW horn arrays at 60 GHz for 360° reconfigurable chip-to-chip communications with interference considerations," *IEEE Trans. Antennas Propag.*, unpublished.

[10] L. Wang, M. Garcia-Vigueras, M. Alvarez-Folgueiras, and J. R. Mosig, "Wideband H-plane dielectric horn antenna," *IET Microw. Antennas Propag.*, vol. 11, no. 12, pp. 1695–1701, Oct. 2017.

[11] P. Baniya, A. Bisognin, K. L. Melde, and C. Luxey, "Chip-to-chip switched beam 60 GHz circular patch planar antenna array and pattern considerations," *IEEE Trans. Antennas Propag.*, vol. 66, no. 4, pp. 1776–1787, Apr. 2018.